Visualization of Flow of Circulating Tumor Cells and Blood Cell Suspensions in Microfluidics

Joseph A. Insley[a,d], Michael C. Hood[b], Jifu Tan[b], Silvio Rizzi[d], Janet Knowles[d], Michael E. Papka[c,d]

[a]*School of Art and Design, Northern Illinois University, Northern Illinois University, DeKalb, IL USA*
[b]*Department of Mechanical Engineering, Northern Illinois University, Northern Illinois University, DeKalb, IL USA*
[c]*Department of Computer Science, Northern Illinois University, DeKalb, IL USA*
[d]*Argonne Leadership Computing Facility, Argonne National Laboratory, Lemont, IL USA*

Abstract

In this work, we present an explanatory visualization of a high-fidelity multiphysics simulation of circulating tumor cell (CTC) capture in a microfluidic device. Detecting rare CTCs in the bloodstream is challenging but important for both clinical diagnostics and fundamental research. Microfluidics showed a great promise in earlier CTC detection. To better understand the transport physics of CTCs in microfluidic devices, a high-performance computational model was used to investigate the role of micropost sizes and intercellular collisions on CTC transport and adhesion within the device. Modeling of both the red blood cells (RBCs) and CTCs was computed as a spring connected network membrane, while adhesion was modeled through pairwise interactive potentials between the CTCs and microposts. The fluid motion was solved by the lattice Boltzmann method, which was coupled with suspended cells by the immersed boundary method (IBM). The visualization clearly shows streamline layers separated by microposts within microfluidic devices. The animation illustrates that, overall, CTCs display transient rolling movements in areas of high shear on microposts and firm adhesion in low-shear areas. The trajectories of CTCs can be seen closely following fluid streamlines at low RBC concentrations but deviating from streamlines at high RBC concentrations due to the intercellular collisions. The visualization also manifests a special zone where cells rarely cross the streamline layer. These behaviors are difficult or even impossible to observe without the use of visualization.

Keywords:
scientific visualization, high performance computing, cancer cell detection, microfluidics

1. Introduction

Cancer cells detached from a primary tumor and entering into the circulatory system are called circulating tumor cells (CTCs). The spreading of these cells throughout the body can lead to metastasis, which accounts for 90% of cancer patient deaths[1, 2]. The ability to detect these CTCs at earlier stages is important for patient diagnostics and treatment. Microfluidics that exploit fluid flow and its interaction with deformable cells are a promising technique in detecting CTCs from patient blood samples[3, 4, 5, 6, 7]. The goal of microfluidics is to allow for selective adhesion of CTCs onto micoposts within the device when a blood sample is flowing through the device. Microposts, also referred to as micropillars, are small obstacles placed in the microfluidic device with the intent of CTC capture through ligand-receptor interaction. If a higher capture efficiency is achieved, researchers can isolate small numbers of CTCs in suspensions with billions of red blood cells (RBCs). However, the capture efficiency depends on many factors, such as the collision frequency of the CTCs with microposts, flow rate, ligand-receptor adhesive strength, deformability of CTCs, and collision from surrounding RBCs. The mechanism of transport and adhesion of CTCs in RBC suspensions in microfluidics under flow is complex and not fully understood.

To better understand the mechanism, a high-performance computational model was employed to investigate the CTC transport and adhesion in RBC suspensions under flow in a microfluidic device. The simulation reproduced the CTC trajectories and preferred adhesion locations compared with microfluidic experiments[8]. The visualization performed in this work provided vivid views of the CTC transport under the endless collision from surrounding RBCs. It revealed a layered flow pattern formed by the microposts and a special region in the microfluidic device where cells barely arrived, which can be used to revise the device design to increase the CTC capture efficiency. The visualization also showed the dynamic flow behavior and the competition between adhesion and hydrodynamic dislodging force on CTCs when they attached to the micropost surfaces.

2. Circulating Tumor Cells

The animation presented in this paper depicts the flow of cells through a microfluidic device. In this section the device, along with the behavior of circulating tumor cells and red blood cells within, is described. Details of the simulations performed are also discussed.

2.1. Science

This type of passive microfluidic device, shown in Fig.1a, relies on specific adhesion between receptors on CTC membrane and ligands coated on the micropost surface to capture CTCs in flow. PC-3 cells (a type of prostate cancer widely used in research), for example, overexpress EpCAM antigens on their surfaces. The receptor density on the cell membrane depends on the subtype of cancer. For instance, cells undergoing epithelial-mesenchymal transition lose the expression of EpCAM and express more mesenchymal markers. To capture PC-3 cells, anti-EpCAM antibodies can be coated on microposts in the microfluidic device to promote adhesion. To capture other types of CTCs, such as SKBR3, anti-HER2 antibodies can be used. The adhesive strength for a bond between EpCAM and anti-EpCAM was about 4.5 pN[9].

Successful capture of CTCs is also influenced by the fluid flow in microfluidic devices. The micropost layout and shape within the device have great influence over how the cells are transported in the flow—the frequency, that is, with which CTCs collide with microposts. Additionally, the layout of the microposts affects stagnant points in the flow where the fluid velocity is zero and CTC adhesion is likely to occur. There are two types stagnation points: divergent stagnation points and convergent stagnation points. Divergent stagnation points are usually located at the leading point on the micropost and facing the incoming flow, while convergent stagnation points are located behind the micropost. Both simulation and experimental results showed that CTCs preferred to adhere to those stagnation points, with more adhesion at the divergent stagnation points. This is probably due to the contribution from a higher fluid pressure to hold CTCs against the micropost. Finally, collisions from RBCs also impact CTCs contact with microposts, which is a pre-step before firm adhesion. At low RBC concentration, simulations showed that CTCs closely follow streamlines. However, at high RBC concentrations, the CTCs trajectories deviated significantly from the steady state streamlines seeded with the initial location of the CTCs.

2.2. Simulation

Modeling biological flows is challenging as it is a multiphysics problem involving fluid flow, large deformation of cells, and the interaction between them. To resolve the fluid flow within the thin lubrication layer between cell membranes, high performance computing of the model is necessary. In this work, both RBCs and CTCs were modeled as a surface membrane based on coarse-grained molecular dynamics[8]. Stretching and dihedral angular potentials were used to model the membrane resistance to stretching and bending. Constant surface area and cellular volume were maintained by harmonic area and volume potentials. The model was implemented in the popular open-source molecular dynamics simulation package LAMMPS (Large-scale Atomic/Molecular Massively Parallel Simulator) [10].

The fluid flow was solved by the lattice Boltzmann method (LBM) that evolves the density distribution functions from which the fluid variables such as velocities and pressure can be calculated. The LBM was selected because of the inherent high performance over massively parallel processors and versatility in handling complex geometries. Its algorithm consists of streaming and collision steps for density distribution functions without expensive solvers for systems of nonlinear equations from other traditional methods such as the finite volume/element/difference method. In this work, Palabos (Parallel Lattice Boltzmann Solver) was used[11]. To couple the fluid and solid, the immersed boundary method (IBM) was used. In the IBM, the nonslip boundary conditions across the interface were implemented through interpolating the solid velocity from the local fluid velocity. Additionally, the solid force induced by deformation was spread out to the fluid.

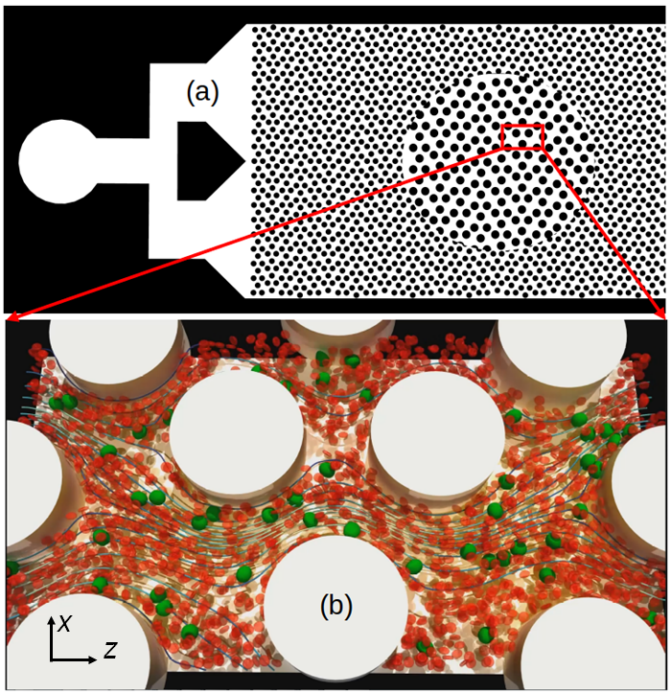

Figure 1: (a) An overview of the microfluidic device with shifted micropost layout. The circular view shows the zoomed-in view. The red box shows a representative unit for computational modeling. (b) Visualization of the simulation with red blood cells (red), cancer cells (green), streamlines (blue), and microposts (white).

Separate simulations were conducted to study the effect of micropost sizes and intercellular collisions on the transport of CTCs in the devices. The domain size of the simulation unit was $260 \times 25 \times 500\,\mu m$ in x, y, z directions, as shown in Fig.1b. The mesh size was $0.5\ \mu m$. This resolution for the discretization of the domain was chosen to allow for acceptable accuracy while minimizing overall computational cost in the study of the effects of different parameters. The single relaxation parameter τ for lattice Boltzmann method was set as $\tau = 1.0$. Initially, 50 cancer cells with a diameter of $12\ \mu m$ were randomly positioned in the microfluidic device, with $12\ \mu m$ being chosen as a representative case for CTC size. A body force of 1.34×10^{-8} in lattice units was used to drive the flow, and periodic boundary conditions in x, z directions were applied. The Reynolds number $Re = 0.004$ defined using the cell diameter and the maxi-

mum fluid velocity. In these studies, each CTC membrane was modeled with 2562 particles, and each RBC was discretized into 642 membrane nodes. Simulations with different RBC volume concentrations were considered: one simulation with 459 RBCs, and another one with 1736 RBCs. The corresponding RBC and CTC volume fractions were 5% and 10%, respectively. The trajectory of the CTCs over time were compared to steady state streamlines in the device. Very little deviation from streamline paths was observed in cases with lower RBC volume fraction and smaller micropost sizes. However, higher RBC volume concentration and larger micropost sizes led to frequent inter-collision of cells, thus impacting the CTC trajectories.

All the simulations were performed on Mira supercomputer at Argonne National Laboratory using our recently developed package[12]. The performance of the code has been tested on Mira, and exhibited near linear scaling from 512 to 8192 processors for both strong and weak scaling tests[12]. For the simulation with a 10% cell volume concentration shown in the animation, it took about 40 hours for 512 processors to run 2.14 million time steps on Mira. All the simulations took about 100,000 core-hours with parametric studies on different cancer cell sizes, RBC concentrations, adhesive strengths, flow rates, and micropost sizes. Detailed simulation parameters and results were reported in Ref.[8]

3. Visualization

Many simulations were performed, with varying parameters, to gain an in-depth understanding of the behavior of the flow of circulating tumor cells within a microfluidic device. This section presents the animation of one representative simulation, and the tools and resources used to produce it. The effectiveness of visualization in capturing the physics of complex fluid and guiding microfluidic design will be demonstrated.

3.1. Animation

An animation of the flow within the device was created to show the overall behavior of the device, see the accompanying video. Simulations were done on a characteristic element of the device, since the whole device is made of many such repeated elements. A snapshot of the simulation is shown in Fig.1b. The microposts are static, with no-slip flow conditions on their boundaries. The streamlines of the fluid are shown as lines that change dynamically over time due to the fluid-cell interactions. The color at any point on a streamline represents the fluid velocity magnitude at that point. Regions of dark blue coloring correspond to smaller velocity magnitudes, while areas of light blue correspond to higher fluid velocity magnitudes. The CTCs and RBCs are shown as green and red membranes, respectively. Periodic boundary conditions are used such that cells exiting from the right or top boundary will re-enter from the left and bottom, and vise versa.

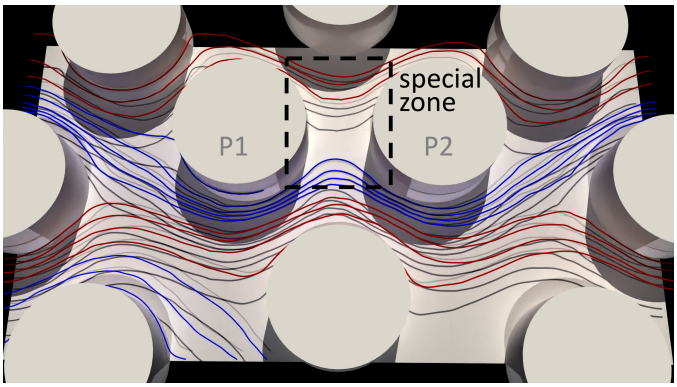

Figure 2: The streamlines at the steady state without any cells show a layered flow pattern in the microfluidic device. A special zone with shorter layer interface between posts P1 and P2 can only be seen through visualization.

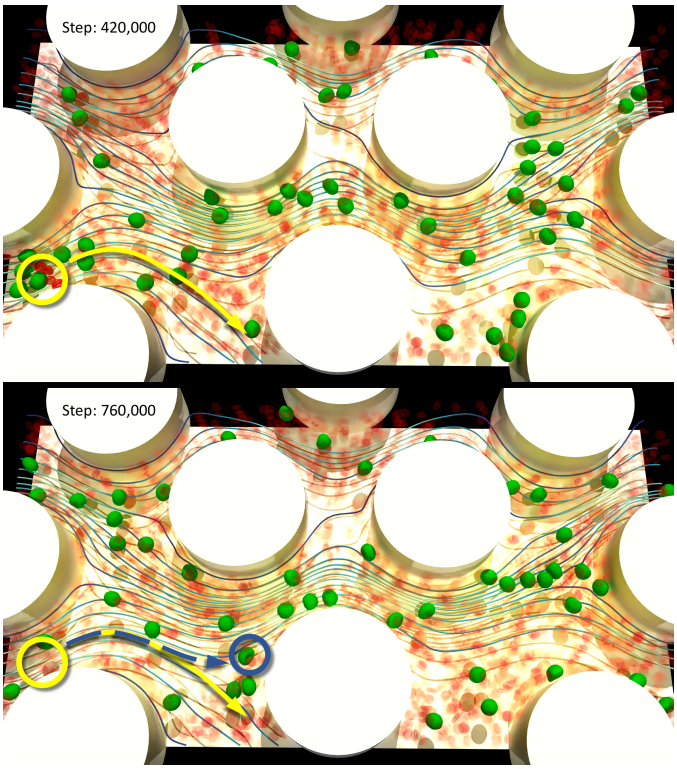

Figure 3: The intercellular collisions on cancer cells lead their trajectories (dashed blue line) to deviate from the steady state streamlines (solid yellow line). Top: time step at $t = 420,000$. Bottom: time step at $t = 760,000$.

Throughout the animation, cells move more quickly when they are away from the microposts, but with no adhesion between cells and microposts. When cells are close to the micropost, the fluid velocity is small, and cell adhesion could occur. After initiating the contact, CTCs showed transient adhesive dynamics, depending on the competition between fluid drag and cell adhesion. At different locations along the surface of microposts, the shear rate is different, thus exerting varying drag forces on CTCs. Regions of fluid with low shear rate primarily occur at stagnation points of the fluid flow. These stagnation points are located at the front and the rear points of a micropost, with respect to the flow direction in the device. Di-

verging and converging fluid flow formed at the front and rear stagnant points, respectively. Cell preferred adhesion sites correspond to these stagnant points. The focus of the visualization is the overall trajectory of cells in the scale of hundreds of micrometers, which is different from small scale adhesion events occurring between nanoscale ligand-receptor interaction on cell membrane and micropost surface. Thus, the adhesion simulation was not shown in the visualization. A separate small scale simulation was used to characterize cell adhesion on a single microposts. The adhesion result from simulation showed great agreements with experiments and were reported in Ref.[8].

Visualizations can help to capture the flow pattern and flow physics, and provide guidance to improve device design. Firstly, it shows the flow pattern in the device can be divided into different layers where the streamlines within each layer were colored by red and blue alternatively, as shown in Fig.2. The layer separation is due to the laminar flow nature in microfluidics. Most of the CTCs started within one layer will stay within the layer. Secondly, the visualization of streamlines showed that there is a special zone in the device where cells barely cross the layer boundary due to the short length of the layer boundary between post P1 and P2, as labeled in Fig.2. The less cell crossing in such region can be clearly seen from the simulation. From design point of view, increasing the separation distance between P1 and P2 or adding a vertical shift between these two posts will enhance the intercellular collision. Thirdly, the intercellular collision did impact the trajectory of the cells. The collision led to further deviation of cell trajectory from its initial streamlines. In particular, when the cell position was close to the separation boundary between the two layers, the cell motion may migrate from one layer to another layer of the flow, depending on which side the collision came from. One example is shown in Fig.3 where the cancer cell would have traveled beneath the middle post at the bottom if it had followed its streamline, as indicated by the yellow arrow in the figure at time step $t = 420,000$. However, the actual trajectory of the cell was pushed upward due to the collision from its surrounding cells, indicated by the dashed blue line in the figure labeled at time step $t = 760,000$.

3.2. Tools and Resources

The visualization was rendered using ParaView[13], enabled with OSPRay[14], a ray tracing-based rendering engine for high-performance, high-fidelity visualization optimized for Intel Architecture CPUs. The instantaneous streamlines, which illustrate the fluid flow through the system were calculated using ParaView. Because the flow field and the cellular data are output on different temporal scales, ParaView is also used to interpolate the flow field for intermediate time steps. The animation consists of nine individual segments, each rendered in parallel using multiple nodes of the Cooley high-performance visualization cluster at the Argonne Leadership Computing Facility. The original soundtrack and narration were composed, recorded, and mixed by the authors. Adobe Premiere was used for post-production to combine the visualizations, annotations, and soundtrack to create the final animation.

Acknowledgment

This research was supported by and used resources of the Argonne Leadership Computing Facility, which is a U.S. Department of Energy Office of Science User Facility operated under contract DE-AC02-06CH11357.

References

[1] D. Wirtz, K. Konstantopoulos, P. C. Searson, The physics of cancer: the role of physical interactions and mechanical forces in metastasis, Nature Reviews Cancer 11 (7) (2011) 512–522.

[2] C. L. Chaffer, R. A. Weinberg, A perspective on cancer cell metastasis, science 331 (6024) (2011) 1559–1564.

[3] S. Nagrath, L. V. Sequist, S. Maheswaran, D. W. Bell, D. Irimia, L. Ulkus, M. R. Smith, E. L. Kwak, S. Digumarthy, A. Muzikansky, et al., Isolation of rare circulating tumour cells in cancer patients by microchip technology, Nature 450 (7173) (2007) 1235–1239.

[4] Y. Wan, Y. Liu, P. B. Allen, W. Asghar, M. A. I. Mahmood, J. Tan, H. Duhon, Y.-t. Kim, A. D. Ellington, S. M. Iqbal, Capture, isolation and release of cancer cells with aptamer-functionalized glass bead array, Lab on a Chip 12 (22) (2012) 4693–4701.

[5] Y. Wan, J. Tan, W. Asghar, Y.-t. Kim, Y. Liu, S. M. Iqbal, Velocity effect on aptamer-based circulating tumor cell isolation in microfluidic devices, The Journal of Physical Chemistry B 115 (47) (2011) 13891–13896.

[6] P. Preira, V. Grandne, J.-M. Forel, S. Gabriele, M. Camara, O. Theodoly, Passive circulating cell sorting by deformability using a microfluidic gradual filter, Lab on a Chip 13 (1) (2013) 161–170.

[7] A. F. Sarioglu, N. Aceto, N. Kojic, M. C. Donaldson, M. Zeinali, B. Hamza, A. Engstrom, H. Zhu, T. K. Sundaresan, D. T. Miyamoto, et al., A microfluidic device for label-free, physical capture of circulating tumor cell clusters, Nature methods 12 (7) (2015) 685–691.

[8] J. Tan, Z. Ding, M. Hood, W. Li, Simulation of circulating tumor cell transport and adhesion in cell suspensions in microfluidic devices, Biomicrofluidics 13 (6) (2019) 064105.

[9] L. S.-L. Cheung, X. Zheng, L. Wang, J. C. Baygents, R. Guzman, J. A. Schroeder, R. L. Heimark, Y. Zohar, Adhesion dynamics of circulating tumor cells under shear flow in a bio-functionalized microchannel, Journal of micromechanics and microengineering 21 (5) (2011) 054033.

[10] S. Plimpton, Fast parallel algorithms for short-range molecular dynamics, Journal of computational physics 117 (1) (1995) 1–19.

[11] J. Latt, O. Malaspinas, D. Kontaxakis, A. Parmigiani, D. Lagrava, F. Brogi, M. B. Belgacem, Y. Thorimbert, S. Leclaire, S. Li, et al., Palabos: Parallel lattice boltzmann solver, Computers & Mathematics with Applications (2020).

[12] J. Tan, T. R. Sinno, S. L. Diamond, A parallel fluid–solid coupling model using lammps and palabos based on the immersed boundary method, Journal of Computational Science 25 (2018) 89–100.

[13] J. Ahrens, B. Geveci, C. Law, Paraview: An end user tool for large data visualization, in: C. Hansen, C. Johnson (Eds.), The Visualization Handbook, Morgan Kaufmann, 2005, pp. 717–731.

[14] I. Wald, G. Johnson, J. Amstutz, C. Brownlee, A. Knoll, J. Jeffers, J. Gunther, P. Navratil, OSPRay - A CPU Ray Tracing Framework for Scientific Visualization, IEEE Transactions on Visualization and Computer Graphics 23 (1) (2017) 931–940. doi:10.1109/TVCG.2016.2599041.
URL https://doi.org/10.1109/TVCG.2016.2599041